≋CHEST®

CrossMark

Tumor Cell Malignant Properties Are Enhanced by Circulating Exosomes in Sleep Apnea

Isaac Almendros, PhD; Abdelnaby Khalyfa, PhD; Wojciech Trzepizur, MD, PhD; Alex Gileles-Hillel, MD; Lei Huang, PhD; Mahzad Akbarpour, PhD; Jorge Andrade, PhD; Ramon Farré, PhD; and David Gozal, MD, FCCP

BACKGROUND: OSA is associated with increased cancer incidence and mortality. Exosomes are vesicles secreted by most cells. They are released into the bloodstream and play a role in tumor progression and metastasis. We evaluated whether the chronic intermittent hypoxia (IH) that characterizes OSA leads to release of tumor-promoting exosomes in the circulation.

METHODS: C57/B6 male mice were randomized to 6 weeks of IH or room air (RA). A subgroup was injected with TC1 lung carcinoma cells in the left flank after 2 weeks of IH. Exosomes from mouse plasma and from 10 adult human patients with OSA before and after treatment for 6 weeks were cocultured with mouse TC1 and human adenocarcinoma cells lines. Malignant tumor properties such as proliferation, migration, invasion, and endothelial monolayer disruption were assessed, as was micro-RNA (miRNA), exosomal content, and transcriptomic effects of exosomes on TC1 cells in vitro to identify target genes.

RESULTS: Application of IH-induced exosomes from either IH-exposed tumor-bearing (IH+) or non-tumor-bearing (IH–) mice significantly promoted TC1 malignant properties. Similarly, before adherent treatment, exosomes from patients with OSA significantly enhanced proliferation and migration of human adenocarcinoma cells compared with after adherent treatment. Eleven distinct miRNAs emerged in IH–exposed mice, and their gene targets in TC1 cells were identified.

CONCLUSIONS: Circulating exosomes released under IH conditions in vivo selectively enhance specific properties of lung tumor cell cultures. Thus, plasma exosomes participate in the increased tumor aggressiveness observed in patients with OSA.

CHEST 2016; 150(5):1030-1041

KEY WORDS: cancer; exosome cargo; exosomes; extracellular vesicles; intermittent hypoxia; microenvironment; miRNA; mRNA; OSA

OSA is a highly prevalent condition that leads to intermittent hypoxia (IH) and sleep fragmentation. OSA has recently been associated with increases in the risk of incident cancer,[1-4] as well as enhanced tumor aggressiveness[5] and cancer-associated mortality.[2,6,7] These epidemiologic findings are further supported by murine experiments, whereby application of IH promoted tumor growth, invasiveness, and risk of metastasis in cancer models and involved altered immune function.[8-10]

Initiation of tumor and its metastatic proliferation involves extraordinarily complex communication between tumor cells and the surrounding environment, including adjacent nontumor cells. Exosomes are small vesicles that are ubiquitously secreted in response to external stimuli; they contain proteins, lipids, messenger RNA (mRNA), and micro-RNA (miRNA) and represent an important mode of intercellular communication through regulated generation and transfer of their cargo to target cells.[11] Exosomes undergo endocytosis by the target cells and deliver their cargo within specific intracellular compartments.[11] Exosomes are currently under intense investigation, since they have been implicated in the modulation of a wide range of malignant processes.[12,13]

Hypoxia can increase exosomal release and selectively modify exosome contents to enhance tumor proliferation and angiogenesis.[14] Based on the aforementioned evidence on the adverse effects of IH on tumor biology,[8,10] we hypothesized that exposure to IH could promote changes in circulating exosomes and that the latter could account, at least in part, for the increased tumor malignant properties observed during IH exposures.

Methods

For a flow diagram of the murine experiments see e-Figure 1.

Cell Lines and Culture Conditions

Mouse epithelial lung tumor cells TC1 (ATCC CRL-2785) and human colonic (HT29) and pancreatic (AsPC-1) adenocarcinoma cells were purchased from Sigma (Sigma-Aldrich) and grown in standard media (e-Appendix 1).

Animals and Experimental Groups

The experimental protocol was approved by the Institutional Animal Care and Use Committee of the University of Chicago (Animal Care and Use Procedure Certificate No. 72190) and was carried out in C57BL/6J 12-week-old male mice obtained from Jackson Laboratories who were exposed to IH or room air (RA) as previously described.[9,15]

Subcutaneous Lung Tumor Model

Mice exposed to either IH or RA were injected with TC1 cells after 2 weeks of treatment (n = 10 each; RA [RA+] or tumor [IH+]). Four weeks after tumor injection, the mice were killed, exsanguinated by cardiac puncture, and plasma samples were collected. Tumors were excised and weighed, and invasiveness was assessed visually and confirmed by histologic analysis, as previously described.[4]

Human Subjects

To examine whether exosome effects induced by IH exposure in mice would be replicated in patients experiencing a sleep disorder associated with IH, plasma samples from 10 patients diagnosed with OSA, using overnight in-laboratory polysomnography, were examined. The mean age was 52.5 ± 6.7 years; seven patients were men; four patients were African American and the rest were white; BMI was 34.7 ± 4.2 kg/m^2; and the apnea-hypopnea index (a measure of OSA severity) was 36.7 ± 8.3 events per hour of sleep (ie, moderate to severe OSA). All the participants provided written informed consent, and the research protocol was approved by the research ethical board at the University of Chicago (protocol No. 10-702-A-CR004). For each patient, blood was collected before CPAP treatment was started, as well as following 6 weeks of adherent CPAP treatment. Adherence to CPAP treatment was defined as using the device at least 6 nights per week for > 5 h per night. In addition, 10 age-, sex-, ethnicity-, and BMI-matched subjects in whom overnight polysomnography results were normal were also assessed (n = 10; age, 51.4 ± 5.8 years; three women; four African Americans; BMI, 33.8 ± 3.9 kg/m^2; apnea-hypopnea index, 2.7 ± 1.4 per hour of sleep). Plasma was isolated from fasting morning peripheral blood samples using centrifugation at $\times 2000$ g for 20 min at 4°C and stored at –80°C until further analysis.

Exosomes

Exosomes were isolated from frozen plasma using standard approaches, as previously reported.[16] Briefly, 200 µL of plasma was collected and centrifuged at $\times 2000$ g for 20 min, and 60 µL of the Total Exosomes Isolation Reagents (Life Technologies) were added. The mixtures were incubated at 4°C for 30 min, followed by centrifugation at $\times 10,000$ g for 5 min. The pellets were suspended in 100 µL of $\times 1$ phosphate-buffered saline and stored at –20°C. In vitro assessments of exosome-induced malignancy consisted of proliferation and migration for both human and murine exosomes and three-dimensional spheroid invasion and transendothelial extravasation assays. In addition, exosome-treated confluent monolayers of bEnd3 endothelial cells (ATCC) were immunostained for ZO-1 tight junction protein (e-Appendix 1).

Source of Exosomes

Isolated exosomes from RA– and IH– were subjected to the ImageStream imaging cytometer (EMD Millipore) for detection of cell sources, as previously described.[16] Absolute counts (objects/mL) were automatically calculated as part of the region statistics, and values were tabulated for each of the populations in each sample (e-Appendix 1).

miRNA and mRNA Microarray Analysis

Total RNA, including miRNA, was isolated from exosomes of IH– and RA–exposed mice (n = 7 per group), and expression analyses were performed using Agilent Microarray Platform (SurePrint G3 8 × 60K) according to manufacturer's instructions (Agilent Technologies) that contain 2,006 miRNAs from miRBase, version 19.[17] RNAs were isolated from TC1 cells treated with exosomes from RA–exposed (n = 6) and IH– (n = 6) mice and hybridized with whole-genome mouse Agilent microarrays. We applied a limma moderated t test to detect differentially expressed genes, considering the batch effect

caused by different arrays as covariates in the linear model. *P* values were adjusted by the Benjamini-Hochberg method.[18] Differentially expressed genes were identified using either a false discovery rate of 0.05 or a log-fold change of 1.5 and false discovery rate of 0.05. To examine the biological function and clustering analysis of the differentially expressed miRNAs, we used DIANA miRPath 3.0 software (e-Appendix 1). Selected genes for mRNAs and miRNAs were validated by quantitative real-time polymerase chain reaction (qRT-PCR) using the 7500 PCR system (Applied Biosystems) according to a standard protocol. The cycle number (Ct) values were averaged, and the difference between the TATA sequence binding protein Ct and the gene of interest Ct were calculated for the relative expression of the gene of interest using the 2-ΔΔCt method.[19] The results are presented as fold change of IH relative to the RA group.

Integrated Analysis of miRNA and mRNA Expression Profiles

Integrated analysis of the miRNA putative targets and mRNA expression profiles derived from TC1 treatments was carried out

using the differentially expressed miRNAs and mRNAs. The mRNAs were initially predicted computationally by miRNA target-prediction programs using miRwalk (http://zmf.umm.uni-heidelberg.de/apps/zmf/mirwalk2/). For the transcription factors in the miRNA-mRNA interaction network, we used AnimalTFDB (www.bioguo.org/AnimalTFDB/download_index.php?spe=Mus%20musculus). These transcription factors were annotated in the miRNA-mRNA interaction networks using mygene (http://mygene.info).[20]

Statistical Analysis

Data are presented as mean ± SE. Tumor growth comparisons between RA and IH groups were carried out by Student *t* tests. For tumor malignancy variables measured in vitro, two-way analysis of variance was conducted with treatment (RA vs IH) and specific outcome measures as variables of interest. The nonparametric Mann-Whitney rank sum test was used for data that were not normally distributed. Two-tailed *P* values were calculated for all pairwise multiple comparison procedures using the Student-Newman-Keuls test among groups. $P < .05$ was defined as achieving statistical significance.

Results

Tumor Growth and Invasiveness

Mice exposed to IH experienced increased tumor growth and invasiveness as previously reported.[9] Specifically, IH led to enhanced tumor weight (IH+: 1.54 ± 0.16 g) when compared with mice injected with TC1 cells after 2 weeks of RA (RA+) exposure (RA+: 0.63 ± 0.15 g; $P = .002$). In addition, IH+ exposure promoted tumor invasion across the capsule to neighboring tissues in all 10 animals, whereas this feature was present in only one of the 10 mice exposed to RA+ ($P < .001$).

Exosome Cell Sources

Exosomes are released into the extracellular space through the endocytic pathway and are characterized by

size, density, and specific protein markers.[21,22] The overall concentrations of plasma-isolated exosomes in IH– mice were significantly increased, and these exosomes were derived from multiple cell sources, including platelets, endothelial cells, endothelial progenitor cells, and monocytes compared with RA– mice, as shown in Figure 1.

IH-Induced Exosomes Increase Tumor Malignancy in Vitro

Application of plasma exosomes isolated from mice exposed to IH promoted increased TC1 malignant properties in vitro (Fig 2). We found that both exosomes from mice exposed to IH without injecting TC1 cells (IH–) and from IH-exposed mice injected with tumors cells (IH+) promoted increased TC1 proliferation

Figure 1 – *Plasma exosome cell sources in mice exposed to either IH or RA using the Image-Stream MkII system. Platelets were identified by expression of CD41 and absence of other markers, such as CD45 and CD144. Leukocytes were identified by their expression of CD45, and that population was further subgated for expression of CD115 to identify monocytes. Endothelial cells were identified by expression of CD144, and EPC additionally expressed CD34. ImageStream data were acquired using INSPIRE and analyzed using IDEAS. Quantification for exosomes from each cell source in IH and RA was performed (n = 6 for each group). * indicates statistical significance between IH– vs RA–, with P = .0001 for platelets; P = .0008 for endothelial cells; P = .001 for EPC; and P = .03 for monocytes. EPC = endothelial progenitor cells; IH = intermittent hypoxia; IH– = IH-exposed mice not injected with tumors cells; IH+ = mice injected with TC1 cells after 2 weeks of IH; NPEC = non-proliferating endothelial cells; RA = room air; RA– = mice not injected with TC1 cells after 2 weeks of RA; RA+ = mice injected with TC1 cells after 2 weeks of RA.*
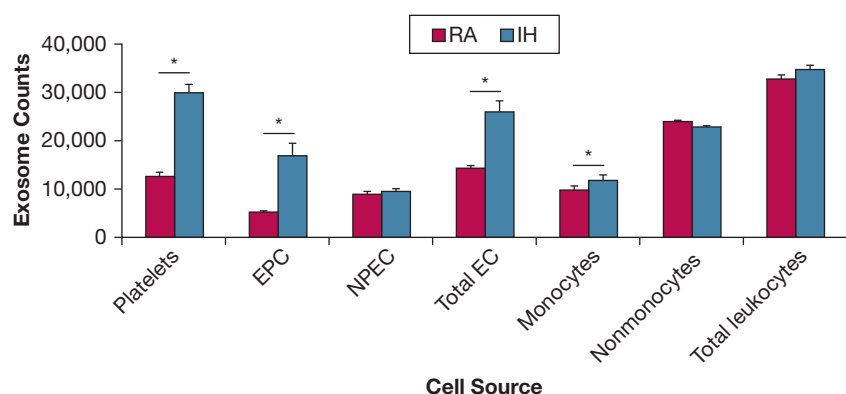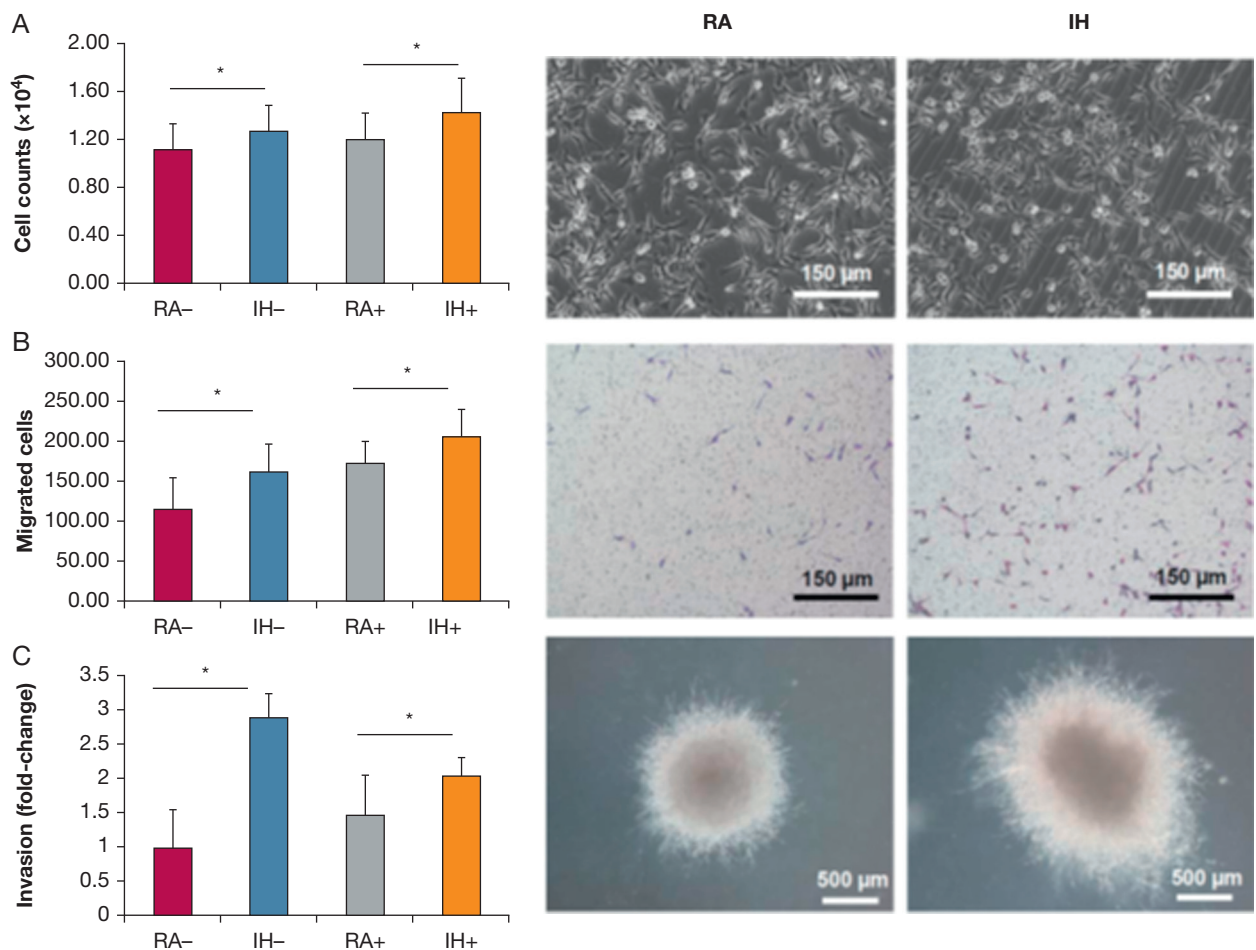
Figure 2 – *Effects of plasma exosomes derived from IH– or IH+ mice on mouse lung TC1 cell on proliferation, migration, and invasion. Malignant properties of TC1 cells exposed to plasma-derived exosomes from tumor (+) and non-tumor-bearing mice (–) exposed to either normoxia (RA) or intermittent hypoxia (IH). Representative images of non-tumor-bearing mice for each variable are shown in the columns on the right. A, The circulating exosomes from mice bearing tumors increased the proliferation of TC1 (n = 7). This increase was further enhanced by IH in the absence and presence of tumor. B, Similarly, the presence of tumor in plasma-derived exosomes induced increases in migration of TC1 cells. The migration was also enhanced by IH in both conditions (tumor vs nontumor) (n = 7). C, The invasion of TC1 cells as assessed by three-dimensional spheroid cultures showed a trend toward increase when exosomes from tumor-bearing mice (n = 5) were compared with normoxic non-tumor-bearing mice. IH exposures significantly increased invasiveness in IH vs RA. Data are presented as mean ± SE. * indicates P < .01. See Figure 1 legend for expansion of abbreviations.*

in vitro (RA+ vs RA–, $P < .04$; IH+ vs IH–, $P = .001$; IH– vs RA–, $P = .03$, and IH+ vs RA+, $P = .001$) (Fig 2A). In migration assays, cocultures of TC1 and exosomes from IH-exposed mice increased their migration compared with those from RA-exposed mice when fetal bovine serum was used as a chemoattractant in the lower chamber of the transwell system (Fig 2B; n = 12 per group). (For comparison, RA+ vs RA–, $P = .01$; IH+ vs IH–, $P = .04$; IH– vs RA–, $P = .02$, and IH+ vs RA+, $P = 0.11$.) For invasion assays, we used three-dimensional spheroid assays, whereby application of exosomes derived from the four groups revealed that the in vivo presence of tumor during IH (IH+ vs IH–, $P = .02$) as well as with IH alone (IH– vs RA–, $P = .001$) (Fig 2C) significantly enhanced invasion.

Disruption of Endothelial Cell Barrier Integrity and Tight Junctions

Next, to test the influence of exosomes on the endothelial cell barrier, we used two different approaches: electric cell-substrate impedance sensing and immunoreactivity for occludin (ZO-1) expression. Plasma exosomes of IH-exposed mice either with (IH+) or without TC1 tumors (IH–) induced greater disruption of the endothelial monolayer barrier integrity compared with RA-derived plasma exosomes (Figs 3A, 3B). Significant comparisons included IH– vs RA–, IH+ vs RA+, and IH+ vs IH– ($P < .01$), whereas the comparison of RA+ vs RA– was not statistically significant. Furthermore, immunostaining of tight junctions with ZO-1 immunosera confirmed the
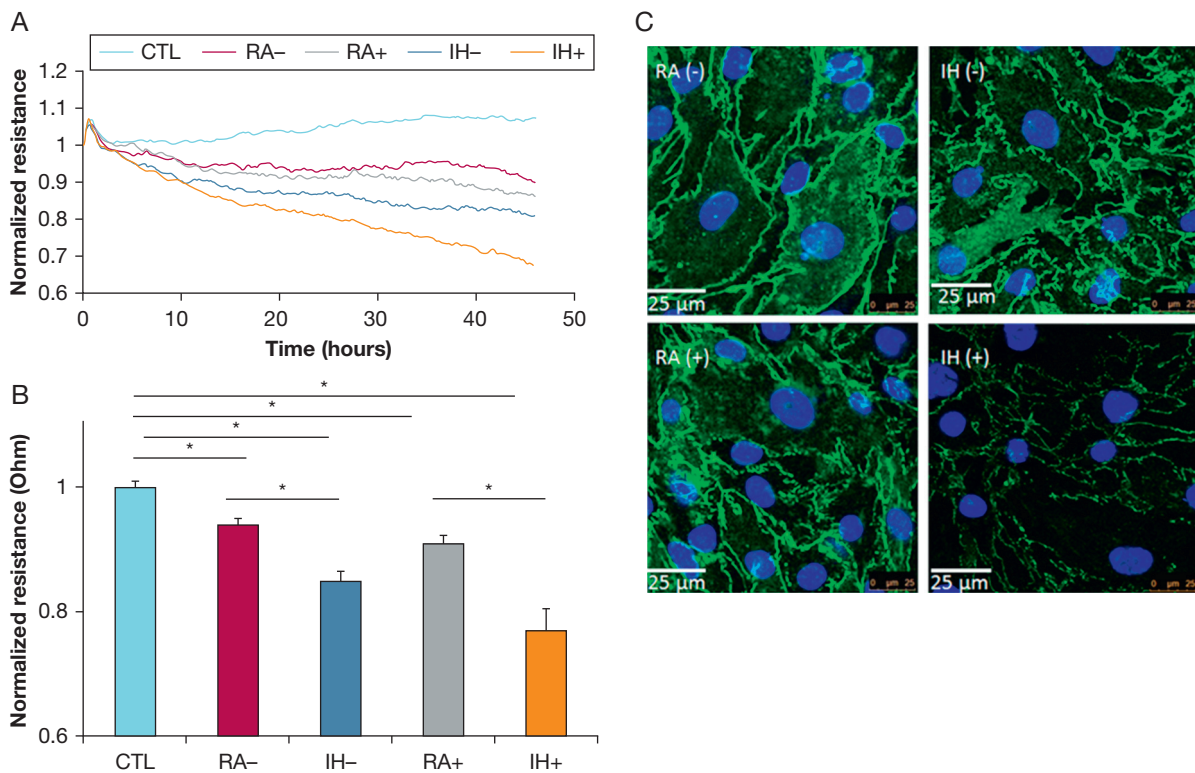
Figure 3 – *Effect of plasma-derived exosomes on electric cell substrate impedance sensing (ECIS) and ZO-1 confocal microscopy imaging. Continuous sampling of endothelial resistance during 40 h after adding exosomes from each condition (A) and mean values at 40 h from each condition (B) after adding exosomes to the confluent endothelial monolayer (A). Plasma-derived exosomes from IH-exposed mice induce increased endothelial cell monolayer disruption compared with exosomes derived from tumor-bearing or non-tumor-bearing mice exposed to RA (n = 8). B, Values recorded at 40 h (P < .001 for IH– vs RA–; P < .0001 for IH+ vs RA+). C, Tight junction protein ZO-1 immunohistochemical results in bEnd3 endothelial cells following treatment with exosomes. Exosomes from IH and RA mice with (+) and without tumors (–) were applied to mouse bEnd3 cells for 24 h. Tight junction protein ZO-1 (green) and nuclei (DAPI blue) were immunostained with corresponding antibodies. C, Representative for RA–, IH–, RA+, and IH+. Disruption of ZO-1 continuity is particularly apparent in IH-exposed mice with and without tumors. Images are representative of n = 7 per group. Scale bar represents 25 µm. CTL = control. See Figure 1 legend for expansion of other abbreviations.*

functional and structural disruption of endothelial tight junctions triggered by IH-derived exosomes (Fig 3C).

Plasma Exosomes from Patients With OSA Increase Proliferation and Migration

Plasma exosomes derived from untreated patients with OSA increased in vitro HT29 and AsPC-1 adenocarcinoma cellular proliferation when compared with either the same patients after 6 weeks of adherent CPAP treatment (n = 10 subjects) (Fig 4) or matched control subjects without OSA (n = 10 per group) (Fig 4). The number of proliferating AsPC-1 cancer cells was also increased when adding exosomes to the transwell chamber for subjects before adherent treatment vs healthy subjects (P = .003), for subjects after adherent treatment vs healthy subjects (P = .005), and for subjects before adherent treatment vs after adherent treatment (P = .01). Similarly, increased migration for colon adenocarcinoma HT29 cells was apparent in subjects

before adherent treatment compared with after adherent treatment (n = 10; P < .01) (Fig 4)) and for pancreatic AsPC-1 cells before adherent treatment vs after adherent treatment (P = .03) (Fig 4). However, we were unable to assess invasion in AsPC-1 because of limited capacity by some of these cell lines to generate three-dimensional spheroids,[23] but we found no significant differences in invasion across HT29-generated three-dimensional spheroids before adherent treatment and after adherent treatment (P < .01).

Exosomal miRNA Expression Profiling

Using miRNA microarrays, we identified 11 highly significant miRNAs (Fig 5) in IH– vs RA–, namely, mmu-miR-671-5p, mmu-miR-6418-5p, mmu-miR-709, mmu-miR-6366, mmu-miR-5100, mmu-miR-2137, mmu-miR-882, mmu-miR-92a-3p, mmu-miR-451a, mmu-miR-3082-5p, and mmu-miR-5113. Of those miRNAs, we validated four miRNAs (two upregulated and two downregulated) using qRT-pCR as indicated
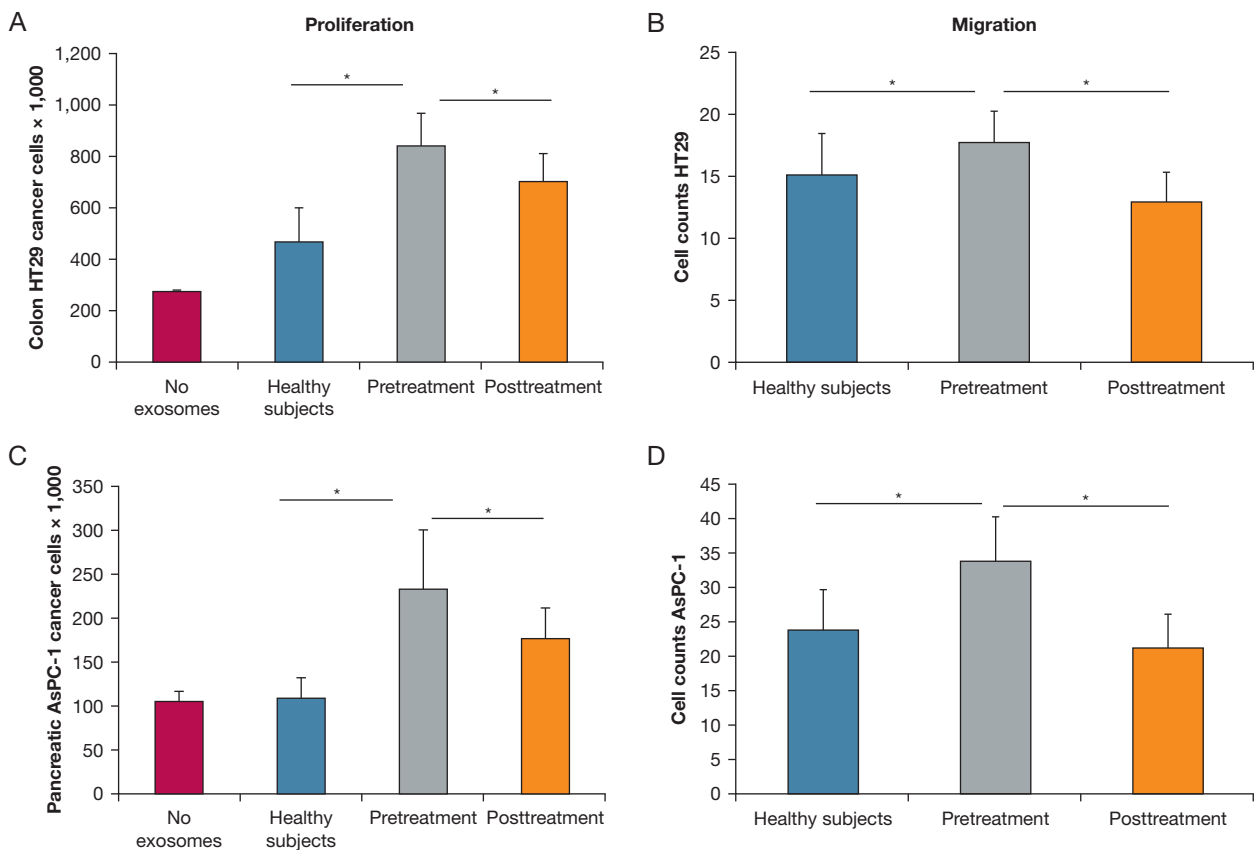
Figure 4 – *Effect of plasma exosomes from patients with OSA before and after CPAP treatment and matched healthy control subjects on proliferation and migration in human colonic and pancreatic adenocarcinoma cell lines in vitro. Exosomes derived from patients diagnosed with OSA before and after 6 weeks of CPAP treatment or from healthy subjects without OSA were incubated in vitro with either (A and B) a human colonic adenocarcinoma cell line or a pancreatic adenocarcinoma cell line (AsPC-1) and induced increased proliferation (A and C) and migration (B and D). Asterisk (*) indicates before adherent treatment vs healthy subjects; P = .001; after adherent treatment vs healthy subjects, P = .04; before adherent treatment vs after adherent treatment, P = .01; n = 10 per experimental group.*

in Table 1. The selected miRNAs exhibited expression levels from qRT-PCR that are consistent with the microarray results, confirming the reliability of the microarray data.

mRNA Expression of Treated TC1 Cells With Plasma Exosomes

To identify TC1 target genes, we used plasma exosomes derived from mice RA– or IH– mice and applied those exosomes to TC1 cells in vitro and identified 2,002 differentially expressed genes, from which a subset was further validated using qRT-PCR (Table 2). In the gene ontology (GO) biological process analysis, the majority of the differentially expressed genes were related to cancer-associated biological behaviors, such as cell cycle control, cell division, and cell proliferation. In the Kyoto Encyclopedia of Genes and Genomes pathway analysis, the majority of exosomal target mRNAs was also found to be involved in cancer-related pathways.

Integrated miRNA-mRNA Target Predictions

Next, we used the mRNA target predictions of the 11 differentially expressed miRNAs and integrated them with the actual mRNAs previously identified from exosome-treated TC1 cells (1,145 genes). Heat map clustering and canonical pathways of differentially expressed genes in plasma exosomes derived from IH– and RA–treated with TC1 cells in vitro are shown in Figure 6. As an illustrative example, some of the pathways involved insulin-like growth factor-1, integrin, and 5'-adenosine monophosphate-activated protein kinase signaling. We also identified the top 50 highly significant differentially expressed genes (e-Table 1) and the overall integrated GO (e-Fig 2). Notably, some of the biological processes in GO analyses include the following: intracellular signaling, guanosine triphosphatase-mediated signaling, and cellular protein metabolic processes. Using Ingenuity Pathway Analysis software, we identified the top networks found
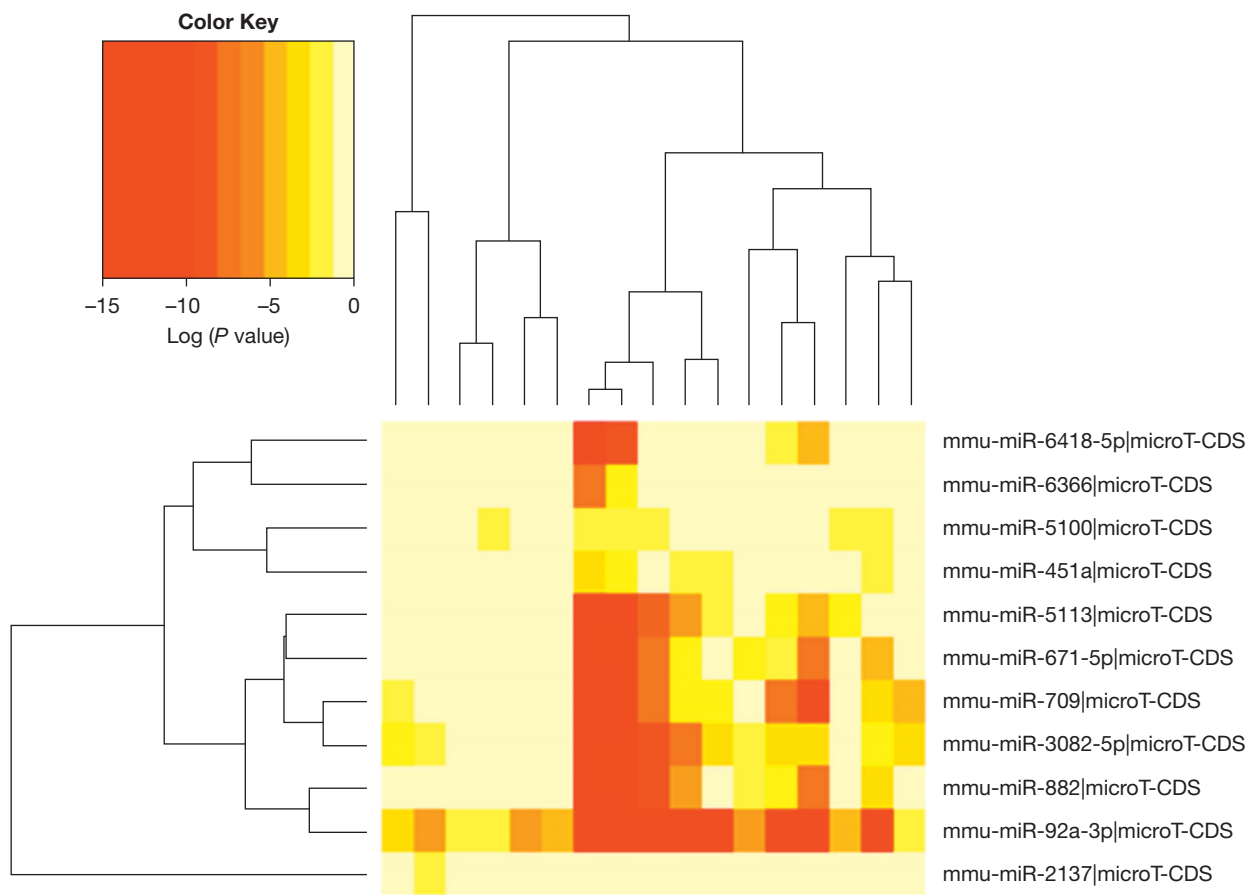
Figure 5 – *Heat map clustering of differentially expressed plasma-derived exosomal micro-RNAs (miRNAs) derived from IH– and RA–. The color key of the heat map represents the P value for the different expression levels of the 11 miRNAs (n = 6 per experimental group). See Figure 1 legend for expansion of abbreviations.*

in IH– vs RA– (Table 3), which included three networks that are involved in cancer biology (boldface in Table 3), and one network that is involved in the inflammatory response (in italics). The networks involved in cancer are also illustrated in more detail in e-Figure 3.

Integrating pathway analysis of potential targets with miRNA expression data is one way to distill a complex data set, and this approach may suggest specific

transcriptional pathways that could be enriched in targets of regulated miRNAs. In such analyses, 246 transcription factors emerged as being associated with the IH– exosomes (e-Table 2). The majority of these transcription factors were associated with the following miRNAs: mmu-miR-671-5p, mmu-miR-6418-5p, mmu-miR-609, mmu-miR-882, mmu-miR-92a-3P, mmu-miR-3082-5p and mmu-miR-5113 (e-Table 2). Some of these transcription factors involved cancer and T-cell

TABLE 1] qRT-PCR Validation Analysis of Differentially Expressed miRNAs in Plasma Exosomes in IH– and RA–

	Microarray		qRT-PCR	
miRNA	Fold Change	P Value	Fold Change	P Value
mmu-miR-92a-3p	2.26 ± 0.46	.01	1.69 ± 0.39	.02
mmu-miR-709	1.25 ± 0.14	.002	1.35 ± 0.21	.03
mmu-miR-671-5p	−1.84 ± 0.42	.0001	−1.53 ± 0.38	.003
mmu-miR-882	−1.65 ± 0.18	.007	−1.48 ± 0.62	.002

IH– = mice exposed to IH not injected with tumors cells; miRNA = micro-RNA; qRT-PCR = real-time polymerase chain reaction; RA– = mice not injected with TC1 cells after 2 weeks of RA.

Gene Symbol	Gene Name	RefSeq	Fold Change			
			Microarray	P Value	qRT-PCR	P Value
Abcf2	ATP-binding cassette, sub-family F	NM_001190443.1	1.82 ± 0.23	1.40E-06	1.56 ± 0.11	.001
Ifi27I2a	Interferon, alpha-inducible protein 27 like 2A	NM_001281830.1	1.52 ± 0.27	4.88E-06	1.25 ± 0.13	.02
Hoxb9	Homeobox B9	NM_008270.2	1.71 ± 0.37	.002	1.25 ± 0.14	.005
Rab37	RAB37, member RAS oncogene family	NM_001163753.1	1.62 ± 0.37	2.3057E-05	1.21 ± 0.11	.003
Eif4g2	Eukaryotic translation initiation factor 4, gamma 2	NM_001040131.2	-1.98 ± 0.36	7.05E-06	−1.78 ± 0.42	.001
Mapk8ip3	Mitogen-activated protein kinase 8 interacting protein 3	NM_001163447.1	-1.45 ± 0.19	9.35E-06	−1.85 ± 0.16	.01

ATP = adenosine triphosphate; RefSeq = reference sequence. See Table 1 legend for expansion of other abbreviations.

function, including forkhead box M1, SMAD family member 1, signal transducer and activator of transcription 6, zinc fingers, metastasis-associated 1, T-cell acute lymphocytic leukemia 1, and tumor growth factor-β-induced factor homeobox 2.

Discussion

In this study, we show that exosomes released during IH mimicking OSA increase the malignancy of TC1 lung tumor cells in vitro. These findings were further confirmed in actual patients with OSA for both colonic and pancreatic adenocarcinoma tumor cells. Over the past few years, exosomes have emerged as critically important players in intercellular communication.

Notably, several studies have demonstrated the role of tumor exosomes in regulating major processes of tumor progression, such as angiogenesis, immune modulation, and metastasis.[24] In a recent study, we showed that IH increases tumor growth and predisposition to metastasis.[9] Here we show that IH leads to increased release of tumor-promoting exosomes that not only enhance tumor cell proliferation and migration but also disrupt the endothelial barrier, thereby facilitating metastatic potential. Similar assessments using exosomes from patients with OSA before and after CPAP treatment and control subjects revealed essentially identical findings in human colonic and pancreatic adenocarcinoma cell lines. We further identified miRNA exosomal cargo differences in IH– that consist of 11 discrete miRNAs,
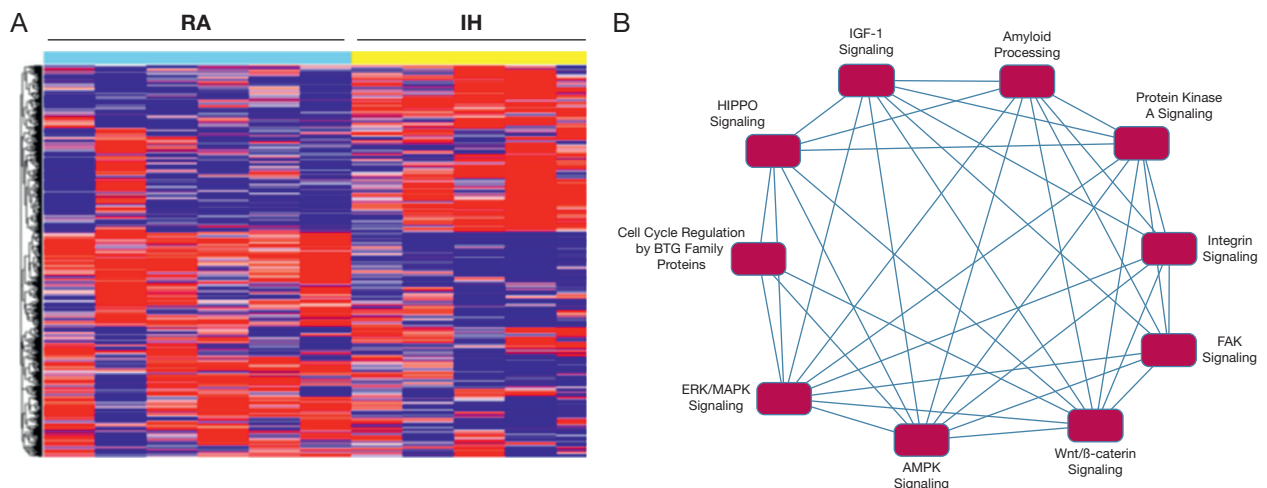

Figure 6 – Heat map cluster for the effects of plasma exosomes derived from IH– and RA– on TC1 cells in vitro. A, Heat map of differentially expressed genes in TC1 cells. The color key above the heat map represents the ranges of P values for expression level differences. B, α list of the most highly statistically significant differences among canonical pathways identified in TC1 cells treated with either IH– or RA– plasma-derived exosomes. IGF-1 = insulin-like growth factor 1. See Figure 1 legend for expansion of other abbreviations.

TABLE 3] List of Top Differentially Expressed Gene Networks Identified From Integration of miRNA Target Genes and Actual mRNA Expression in TC1 Cells in IH– vs RA–

ID	Top Diseases and Functions	Score	Focus Molecules
1	RNA posttranscriptional modification, protein synthesis, developmental disorders	46	35
2	RNA posttranscriptional modification, cell death and survival, cell signaling	46	35
3	**Cancer, hematologic disease, immunologic disease**	43	34
4	RNA posttranscriptional modification, cell morphology, cellular compromise	43	34
5	Infectious diseases, lipid metabolism, molecular transport	43	34
6	Embryonic development, organismal development, cellular assembly and organization	41	35
7	Carbohydrate metabolism, cardiovascular disease, connective tissue disorders	41	33
8	Carbohydrate metabolism, small molecule biochemistry, embryonic development	41	33
9	Cellular compromise, cell cycle, cellular assembly and organization	38	32
10	Cellular assembly and organization, cellular compromise, cellular growth and proliferation	38	32
11	DNA replication, recombination, and repair, gene expression, cellular assembly and organization	37	32
12	*Immunologic disease, inflammatory disease, inflammatory response*	36	31
13	Nervous system development and function, organ morphology, organismal development	36	31
14	Cell cycle, cellular development, embryonic development	36	31
15	Cell morphology, cellular assembly and organization, cellular movement	36	31
16	Carbohydrate metabolism, molecular transport, lipid metabolism	33	30
17	Posttranslational modification, hereditary disorder, lipid metabolism	33	30
18	**Cancer, connective tissue disorders, developmental disorders**	32	33
19	**Lipid metabolism, small-molecule biochemistry, cancer**	32	29
20	Carbohydrate metabolism, lipid metabolism, small-molecule biochemistry	32	29
21	Cellular assembly and organization, cell-to-cell signaling and interaction	32	29
22	Gene expression, RNA posttranscriptional modification, connective tissue disorders	30	28
23	Gene expression, protein synthesis, cellular development	30	28
24	Cellular development, cellular growth and proliferation, organ development	29	28
25	Posttranslational modification, carbohydrate metabolism, lipid metabolism	28	27

Boldface indicates networks involved in cancer biology. Italics indicates network involved in inflammatory response. mRNA= messenger RNA. See Table 1 legend for expansion of other abbreviations.

whereby exploration of their potential gene targets in TC1 tumor cells uncovered 1,145 genes that encode for multiple cancer-related pathways and inflammation.

Growing evidence suggests that hypoxia is an important component of tumor malignant properties, facilitating cancer spread through multiple pathways.[25-27] The microenvironment of solid tumors is characterized by areas of hypoxia that arise during tumor expansion when vessels cannot meet the increasing demand for oxygen. IH has a wide range of physiological responses, including the upregulation of hypoxia-inducible genes, and acts as a source of reactive oxygen species, promoting inflammation and apoptosis at the tissue and cellular levels,[28] where it can also induce metabolic changes.[29] The oxygenation swings produced by IH are translated at the tissue level,[30] including in well-perfused areas within the tumor.[31] In tumor-bearing mice,

application of IH increased tumor growth and invasiveness and altered tumor stromal immunity.[8,9,32] These changes during IH are relevant, since macrophages provide an important source of tumor-inducing exosomes.[33]

This study provides an additional mechanism that can contribute to the increased tumor incidence and malignancy observed in patients with severe OSA.[1,2,4-6,34] Despite the multiplicity of confounders in patient cohorts, studies have shown that measures such as the oxygen desaturation index are independent factors associated with adverse outcomes of cancer.[1,5-7] Thus, the increased tumor malignancy promoted by IH-derived exosomes could have implications in cancer incidence and prognosis in patients with OSA, facilitating the growth and establishment of a primary tumor, as well as increasing the malignant properties of the cancer cells once the tumor

is established. Indeed, several studies have shown that hypoxia increases exosome secretion from several cancer types, including breast,[35] multiple myeloma,[36] prostate,[37] and glioma.[38] These exosomes and microvesicles induced by hypoxia can stimulate angiogenesis,[36,38] stemness,[37] invasiveness,[37] and metastasis.[39] Wang et al[40] showed that naive breast cancer cells incubated with hypoxia-induced microvesicles promotes focal adhesion formation, invasion, and metastasis. Other reports showed increased microvesicle and exosome shedding in response to hypoxia that is mediated in part by processes involving hypoxia-inducible factor-dependent expression.[35,40]

In the absence of IH, our experiments showed that the presence of a tumor provides a source of exosomes that facilitates its growth and enables it to escape immunosurveillance.[41] Tumor-derived exosomes have been shown to promote fibroblast secretion of proangiogenic factors through receptor transfer between the tumor cell and its target,[42] and this exosomal secretion is one of the mechanisms through which tumor cells can communicate with, and reprogram, their microenvironment.[43]

The cell sources of exosomes exhibiting differential effects are varied and predominantly originate from endothelial cells, endothelial cell progenitors, and inflammatory cells. Cell signaling events between endothelial cells, endothelial progenitors, and stromal cells is crucial for the establishment and maintenance of microvascular integrity and has been shown to involve exosomes.[44] Our results suggest that among exosomal cell sources, endothelial cells, endothelial cell progenitors, and inflammatory cells were more abundantly represented in IH and likely constitute the major source of the differences in tumor cell properties delineated herein. Exosomes are also able to govern the function of remote cells by secreting their cargos and reaching cells distant from their site of origin,[45] and in fact, exosomes play a major role in the circulation of miRNAs. Exosomes are involved in the genetic transfer of specific miRNAs that enhance the invasive potential of several breast cancer cell lines.[33] Furthermore, the tumor cell microenvironment is influenced by a wide range of biological components that are expressed and released by the tumor during the development and progression of cancer to promote its growth and metastatic progression.[46,47] Exosomes released by tumor cells can interact with target cells by a number of mechanisms including (1) direct stimulation of the target by surface-expressed ligands, (2) receptor transfer between the tumor cell and the target, (3) horizontal transfer of genetic information to the target, and (4) direct stimulation of the target cell by endocytically expressed surface receptors. Since increasing evidence indicates that the effect of exosomes on target cells is mainly dependent on their intravesicular miRNA expression,[48] we explored the miRNA content in exosomes using unbiased miRNA array approaches and identified 11 differentially expressed miRNAs, which are likely a critical component of their different effects on various tumor cell functions. Regarding their tumor cell targets, several canonical pathways emerged, and included 5'-adenosine monophosphate-activated protein kinase, which plays a key role as a master regulator of cellular energy homeostasis. The kinase is activated in response to stresses that deplete cellular adenosine triphosphate supplies, such as low glucose levels, hypoxia, ischemia, and heat shock.[49,50] In addition, Hippo signaling is an evolutionarily conserved pathway that controls organ size by regulating cell proliferation, apoptosis, and stem cell self-renewal. In addition, dysregulation of the Hippo pathway contributes to cancer development.[51,52] We also, identified 25 IH–modified networks, with three of these networks being involved in cancer biology (e-Fig 2), as well as multiple transcription factors, lending further credence to the intricate role of circulating exosomes in tumor biology.

This study has several limitations. First, the IH model mimics only one of the constitutive elements of sleep disorders such as OSA and does not capture the whole spectrum of perturbations associated with this sleep disorder. Nevertheless, the fact that IH elicits altered exosome miRNA content and selectively enhances specific properties of tumor biology provides a strong impetus and rationale for future studies in both mice and humans. Such studies will have to identify additional elements of exosome cargo that are affected by OSA, including confounders, and since the present study focused exclusively on miRNAs, such studies will also have to explore other functional cargo elements such as mRNAs, proteins, lipids, and DNA. Finally, the specific functionalities of each of the 11 miRNAs in tumor biology will have to be specifically investigated using miRNA mimics and inhibitors, not only to uncover the mechanistic aspects of IH-induced modifications in cancer cell proliferation and migration but also to develop potential therapeutic targets. In this context, our preliminary findings in patients with OSA may enable future implementation of this approach for designing precision in vitro reporter assays and interventions.

Conclusions

Tumor progression results from active partnerships between the tumor and the microenvironment, which would be impossible without efficient modes of exchanging information: direct cell-to-cell contact, secretion of signaling molecules, and release of vesicles such as exosomes into the extracellular space.[53] In this study, we not only confirmed our previous findings that IH increases tumor proliferation, migration, and invasion in vivo but also showed that circulating plasma exosomes obtained from either mice exposed to IH or from patients with OSA enhance tumor cell line proliferation and migration in vitro, indicating that these exosomes may serve as vehicles of intercellular communication that underlie adverse cancer prognosis in the context of perturbed sleep. We also identified a unique set of exosomal miRNAs in IH-exposed mice that further raise the possibility that tumor cells and surrounding stroma may be altered through transfer of exosomal miRNAs. There is no doubt that improved understanding of the complex network of genes and cellular signaling transduction pathways regulated by exosomal miRNAs in the context of OSA will augment our knowledge about its potential deleterious effects among cancer patients.

References

1. Campos-Rodriguez F, Martinez-Garcia MA, Martinez M, et al. Association between obstructive sleep apnea and cancer incidence in a large multicenter Spanish cohort. *Am J Respir Crit Care Med*. 2013;187(1):99-105.

2. Marshall NS, Wong KK, Cullen SR, et al. Sleep apnea and 20-year follow-up for all-cause mortality, stroke, and cancer incidence and mortality in the Busselton Health Study cohort. *J Clin Sleep Med*. 2014;10(4):355-362.

3. Chatsuriyawong S, Gozal D, Kheirandish-Gozal L, et al. Genetic variance in nitric oxide synthase and endothelin genes among children with and without endothelial dysfunction. *J Transl Med*. 2013;11(227):1-11.

4. Chen JC, Hwang JH. Sleep apnea increased incidence of primary central nervous system cancers: a nationwide cohort study. *Sleep Med*. 2014;15(7): 749-754.

5. Martinez-Garcia MA, Martorell-Calatayud A, Nagore E, et al. Association between sleep disordered breathing and aggressiveness markers of malignant cutaneous melanoma. *Eur Respir J*. 2014;43(6):1661-1668.

6. Nieto FJ, Peppard PE, Young T, et al. Sleep-disordered breathing and cancer mortality: results from the Wisconsin Sleep Cohort Study. *Am J Respir Crit Care Med*. 2012;186(2):190-194.

7. Martinez-Garcia MA, Campos-Rodriguez F, Duran-Cantolla J, et al. Obstructive sleep apnea is associated with cancer mortality in younger patients. *Sleep Med*. 2014;15(7):742-748.

8. Almendros I, Montserrat JM, Ramirez J, et al. Intermittent hypoxia enhances cancer progression in a mouse model of sleep apnoea. *Eur Respir J*. 2012;39(1): 215-217.

9. Almendros I, Wang Y, Becker L, et al. Intermittent hypoxia-induced changes in tumor-associated macrophages and tumor malignancy in a mouse model of sleep apnea. *Am J Respir Crit Care Med*. 2014;189(5):593-601.

10. Almendros I, Montserrat JM, Torres M, et al. Intermittent hypoxia increases melanoma metastasis to the lung in a mouse model of sleep apnea. *Respir Physiol Neurobiol*. 2013;186(3):303-307.

11. Raposo G, Stoorvogel W. Extracellular vesicles: exosomes, microvesicles, and friends. *J Cell Biol*. 2013;200(4):373-383.

12. Tickner JA, Urquhart AJ, Stephenson SA, et al. Functions and therapeutic roles of exosomes in cancer. *Front Oncol*. 2014; 4(127):1-8.

13. De Toro J, Herschlik L, Waldner C, et al. Emerging roles of exosomes in normal and pathological conditions: new insights for diagnosis and therapeutic applications. *Front Immunol*. 2015;6(203):1-12.

14. Belting M, Christianson HC. Role of exosomes and microvesicles in hypoxia-associated tumour development and cardiovascular disease. *J Intern Med*. 2015;278(3):251-263.

15. Fung JW, Li TS, Choy DK, et al. Severe obstructive sleep apnea is associated with left ventricular diastolic dysfunction. *Chest*. 2002;121(2):422-429.

16. Khalyfa A, Kheirandish-Gozal L, Khalyfa AA, et al. Circulating plasma extracellular microvesicle miRNA cargo and endothelial dysfunction in OSA children [published online ahead of print May 10, 2016]. *Am J Respir Crit Care Med*. http://dx.doi.org/10.1164/rccm.201602-0323OC.

17. Bolstad BM, Irizarry RA, Astrand M, et al. A comparison of normalization methods for high density oligonucleotide array data based on variance and bias. *Bioinformatics*. 2003;19(2):185-193.

18. Benjamini Y, Hochberg Y. Controlling the false discovery rate: a practical and powerful approach to multiple testing. *J R Stat Soc Series B Stat Methodol*. 1995; 57:289-300.

19. Schmittgen TD, Livak KJ. Analyzing real-time PCR data by the comparative C(T) method. *Nat Protoc*. 2008;3(6):1101-1108.

20. Wu C, Macleod I, Su AI. BioGPS and MyGene.info: organizing online, gene-centric information. *Nucleic Acids Res*. 2013;41:D561-D565.

21. Thery C, Ostrowski M, Segura E. Membrane vesicles as conveyors of immune responses. *Nat Rev Immunol*. 2009;9(8):581-593.

22. Simons M, Raposo G. Exosomes—vesicular carriers for intercellular communication. *Curr Opin Cell Biol*. 2009;21(4):575-581.

23. Sipos B, Moser S, Kalthoff H, et al. A comprehensive characterization of pancreatic ductal carcinoma cell lines: towards the establishment of an in vitro research platform. *Virchows Arch*. 2003; 442(5):444-452.

24. Quail DF, Joyce JA. Microenvironmental regulation of tumor progression and

metastasis. *Nat Med*. 2013;19(11): 1423-1437.

25. Bao B, Azmi AS, Ali S, et al. The biological kinship of hypoxia with CSC and EMT and their relationship with deregulated expression of miRNAs and tumor aggressiveness. *Biochim Biophys Acta*. 2012;1826(2):272-296.

26. Keith B, Simon MC. Hypoxia-inducible factors, stem cells, and cancer. *Cell*. 2007;129(3):465-472.

27. Palazon A, Aragones J, Morales-Kastresana A, et al. Molecular pathways: hypoxia response in immune cells fighting or promoting cancer. *Clin Cancer Res*. 2012;18(5):1207-1213.

28. Almendros I, Wang Y, Gozal D. The polymorphic and contradictory aspects of intermittent hypoxia. *Am J Physiol Lung Cell Mol Physiol*. 2014;307(2):L129-L140.

29. Carreras A, Zhang SX, Almendros I, et al. Resveratrol attenuates intermittent hypoxia-induced macrophage migration to visceral white adipose tissue and insulin resistance in male mice. *Endocrinology*. 2015;156(2):437-443.

30. Almendros I, Farre R, Planas AM, et al. Tissue oxygenation in brain, muscle, and fat in a rat model of sleep apnea: differential effect of obstructive apneas and intermittent hypoxia. *Sleep*. 2011;34(8):1127-1133.

31. Almendros I, Montserrat JM, Torres M, et al. Obesity and intermittent hypoxia increase tumor growth in a mouse model of sleep apnea. *Sleep Med*. 2012;13(10): 1254-1260.

32. Almendros I, Gileles-Hillel A, Khalyfa A, et al. Adipose tissue macrophage polarization by intermittent hypoxia in a mouse model of OSA: effect of tumor microenvironment. *Cancer Lett*. 2015; 361(2):233-239.

33. Yang M, Chen J, Su F, et al. Microvesicles secreted by macrophages shuttle invasion-potentiating microRNAs into breast cancer cells. *Mol Cancer*. 2011;10(117): 1-13.

34. Chang WP, Liu ME, Chang WC, et al. Sleep apnea and the subsequent risk of breast cancer in women: a nationwide population-based cohort study. *Sleep Med*. 2014;15(9):1016-1020.

35. King HW, Michael MZ, Gleadle JM. Hypoxic enhancement of exosome release by breast cancer cells. *BMC Cancer*. 2012;12(421):1-10.

36. Umezu T, Tadokoro H, Azuma K, et al. Exosomal miR-135b shed from hypoxic multiple myeloma cells enhances angiogenesis by targeting factor-inhibiting HIF-1. *Blood*. 2014;124(25):3748-3757.

37. Ramteke A, Ting H, Agarwal C, et al. Exosomes secreted under hypoxia enhance invasiveness and stemness of prostate cancer cells by targeting adherens junction molecules. *Mol Carcinog*. 2015; 54(7):554-565.

38. Kucharzewska P, Christianson HC, Welch JE, et al. Exosomes reflect the hypoxic status of glioma cells and mediate hypoxia-dependent activation of vascular cells during tumor development. *Proc Natl Acad Sci U S A*. 2013;110(18): 7312-7317.

39. Park JE, Tan HS, Datta A, et al. Hypoxic tumor cell modulates its microenvironment to enhance angiogenic and metastatic potential by secretion of proteins and exosomes. *Mol Cell Proteomics*. 2010;9(6):1085-1099.

40. Wang T, Gilkes DM, Takano N, et al. Hypoxia-inducible factors and RAB22A mediate formation of microvesicles that stimulate breast cancer invasion and metastasis. *Proc Natl Acad Sci U S A*. 2014;111(31):E3234-E3242.

41. Yang C, Robbins PD. The roles of tumor-derived exosomes in cancer pathogenesis. *Clin Dev Immunol*. 2011;30(2011):1-11.

42. Muralidharan-Chari V, Clancy JW, Sedgwick A, et al. Microvesicles: mediators of extracellular communication during cancer progression. *J Cell Sci*. 2010;123(10):1603-1611.

43. Barcellos-Hoff MH, Lyden D, Wang TC. The evolution of the cancer niche during multistage carcinogenesis. *Nat Rev Cancer*. 2013;13(7):511-518.

44. Pitchford SC, Furze RC, Jones CP, et al. Differential mobilization of subsets of progenitor cells from the bone marrow. *Cell Stem Cell*. 2009;4(1):62-72.

45. Azmi AS, Bao B, Sarkar FH. Exosomes in cancer development, metastasis, and drug resistance: a comprehensive review. *Cancer Metastasis Rev*. 2013;32(3-4): 623-642.

46. Al-Nedawi K, Meehan B, Rak J. Microvesicles: messengers and mediators of tumor progression. *Cell Cycle*. 2009;8(13): 2014-2018.

47. Iero M, Valenti R, Huber V, et al. Tumour-released exosomes and their implications in cancer immunity. *Cell Death Differ*. 2008;15(1):80-88.

48. Diehl P, Fricke A, Sander L, et al. Microparticles: major transport vehicles for distinct microRNAs in circulation. *Cardiovasc Res*. 2012;93(4):633-644.

49. Canto C, Auwerx J. AMP-activated protein kinase and its downstream transcriptional pathways. *Cell Mol Life Sci*. 2010;67(20):3407-3423.

50. Carling D, Mayer FV, Sanders MJ, et al. AMP-activated protein kinase: nature's energy sensor. *Nat Chem Biol*. 2011;7(8): 512-518.

51. Badouel C, McNeill H. SnapShot: The hippo signaling pathway. *Cell*. 2011;145(3): 484-484.e1.

52. O'Hayre M, Degese MS, Gutkind JS. Novel insights into G protein and G protein-coupled receptor signaling in cancer. *Curr Opin Cell Biol*. 2014;27: 126-135.

53. Kucharzewska P, Belting M. Emerging roles of extracellular vesicles in the adaptive response of tumour cells to microenvironmental stress. *J Extracell Vesicles*. 2013;2(20304):1-7.